ELSEVIER

October 1997

Materials Letters 32 (1997) 295–300

MATERIALS LETTERS

Properties of thoria–yttria solid electrolytes prepared by the citrate technique

I.C. Cosentino, R. Muccillo *

Instituto de Pesquisas Energéticas e Nucleares, Comissão Nacional de Energia Nuclear, C.P. 11049, Pinheiros, 05422-970, S. Paulo, S.P., Brazil

Received 20 January 1997; accepted 26 January 1997

Abstract

Reactive ThO_2:9 mol% Y_2O_3 powders with submicron average particle size have been obtained by the citrate technique. Pressing and sintering at 1550°C/2 h produced pellets with larger than 90% of the theoretical density. X-ray diffractometry and impedance spectroscopy analyses show that a solid solution has been attained. After pressing and sintering the material behaves as an oxygen ion conducting solid electrolyte. Results on ThO_2:Y_2O_3 prepared by the conventional solid state synthesis are also reported for comparison purposes.

PACS: 81.05.Je; 84.37.+q

Keywords: Solid electrolytes; Thoria–yttria; Citrate technique; Impedance spectroscopy; Low sintering temperature

1. Introduction

Ceramic zirconium oxide-based solid electrolytes find large applications in devices for the determination of oxygen dissolved in molten steels, and oxygen content in exhaust tubes of combustion engines [1]. Other applications include solid oxide fuel cells for alternative electrical energy production [2]. Several devices having ZrO_2:Y_2O_3, ZrO_2:MgO and ZrO_2:CaO ceramic electrolytes are readily available commercial products. Thorium oxide, on the other hand, has long been a candidate for solid electrolyte matrix to be used as electrochemical transducer in oxygen sensing devices. Comparing with zirconium oxide, from the processing point of view, it has the advantage of structural phase thermodynamical stability from room temperature to conventional sintering temperatures (80% of its melting point). Zirconium oxide presents the well-studied monoclinic-tetragonal-cubic phase transformations and has to be partially (with monoclinic and cubic/tetragonal phases) or fully (cubic/tetragonal) stabilized by solid solution formation with aliovalent metal oxides to avoid cracking during sintering due to volume change during phase transformations. Even though an improvement in thermal shock resistance and toughening is achieved, problems may arise related to thermal aging due to the thermodynamical metastability of the (ionic conductive) stabilized cubic phase at the temperature of operation of the devices (600°C to 1000°C). The main disadvantages of thorium oxide are the high temperatures required for sintering to obtain solid solutions, as for example 1400°C for

* Corresponding author. Fax: +55-11-8169370.

PII S0167-577X(97)00052-9

pre-sintering and 2200°C for sintering [3], or 1850°C/5 h in flowing hydrogen [4]. Moreover, even though thorium oxide is a low radioactive compound (half-life 1.4×10^{10} years) and used in many available commercial products, the presence of such activity may restrict its widespread application [5]. ThO_2:Y_2O_3 solid electrolytes have already been used in oxygen sensors for monitoring sodium oxide formation in stainless steel vessels containing liquid sodium for heat transfer in liquid metal fast breeder reactors [6] and in solid state galvanic cells for oxygen potential measurements in nuclear reactor environments [7].

In this work a chemical route is followed to prepare reactive ThO_2:Y_2O_3 powders that, after forming, could be sintered at temperatures lower than the conventional ones. Similar results have been recently reported for zirconia–magnesia solid electrolytes prepared at this laboratory following the same technique [8]. Electrochemical impedance spectroscopy analysis was carried out to monitor bulk and grain boundary contributions to the electrical conductivity and as a tool for detecting solid solution formation, assuming that solid solution implies to increasing oxygen vacancy concentration and, consequently, the bulk conductivity. ThO_2:Y_2O_3 solid solutions are known to retain single-phase defective fluorite structure up to $\cong 40$ mol% Y_2O_3 and yttrium ions to substitute for thorium ions promoting fully ionized oxygen vacancies as the compensating defect [9]. Electrochemical impedance studies of symmetrical cells based on yttria-doped thoria were already reported [10]. Three semicircles were detected in the impedance diagrams in the 0.01 Hz–500 kHz frequency range, the one in the high frequency region being assigned to bulk conduction and the other two, at lower frequencies, to interfacial phenomena. More recently, impedance diagrams of ThO_2–15 mol% $YO_{1.5}$ from 10 to 10^5 Hz at temperatures 300–427°C in air have been reported [4]. The specimens were prepared by the oxalate route and sintered at 1850°C for 5 h in flowing hydrogen to obtain high density transparent samples. Cerium-doped thoria specimens have been prepared by co-precipitating thorium and cerium oxalate from an aqueous nitrate solution. Pressed disks achieved 99% of the theoretical density after sintering at 1700°C for 24 h [11].

Here we report impedance diagrams in the 10 Hz–13 MHz frequency range in specimens prepared by the citrate route and sintered at 1550°C for 2 h. The main results show that the citrate route is an useful technique to obtain reactive sinterable thoria–yttria solid solution powders, i.e., powders that after pressing and sintering behave as oxygen-ion conducting solid electrolytes.

2. Experimental

Thorium oxide powders have been obtained after calcination of thorium oxalate produced at a Pilot Plant at this Institute. Yttrium oxide of commercial origin has been dissolved in thorium oxide following the citrate technique. The experimental sequence is the following: citric acid and ethylene glycol (60:40 wt% ratio) are added to a mixture of thorium nitrate and yttrium nitrate for the desired stoichiometry of thoria–yttria solid electrolytes; the temperature bath, kept at 60°C, is raised to 110°C for NO_2 elimination producing a brownish resin; the resin-to-oxide transformation is done in two steps: calcination at 400°C/6 h in air, yielding a black powder, followed by annealing at 800°C/24 h under oxygen for carbon elimination and solid solution formation, yielding a white powder. Specimens with the same starting compositions as the ones prepared by the citrate technique have been prepared by conventional solid state synthesis, namely, mixing, grinding, pressing and sintering. Particle size analyses have been carried out in the powders with a 5100 micromeritics sedigraph analyzer and a CILAS granulometer. Powder suspensions have been prepared for observations in a JEOL JEM200C transmission electron microscope for the determination of average particle size and degree of particle agglomeration. Solid electrolyte pellets were prepared as 10 mm in diameter by 2 mm thickness discs by cold pressing the powders uniaxially at 150 MPa followed by sintering at 1550°C/2 h in air. The apparent densities of the sintered ceramic pellets have been evaluated by the Archimedes method (immersion in water). Phase analysis has been done by X-ray diffractometry with a PW3710 Philips diffractometer. The pellets had their surfaced polished with diamond paste (down to 1 μm) and chemically etched with boiling phospho-

ric acid followed by a thermal etching at 1500°C/30 min to study morphological aspects of the grains in a Philips XL30 scanning electron microscope. Electrical characterization was done by Electrochemical impedance spectroscopy in the 10 Hz–13 MHz frequency range from 250°C to 600°C with a 4192A Hewlett Packard LF impedance analyzer connected via HPIB to a series 900 Hewlett Packard controller. A sample chamber with three specimen holders made of inconel 600, alumina and platinum electrodes and leads has been built. The temperature of the specimens has been determined within 0.5°C accuracy with a S-type Pt/Pt–Rh thermocouple with its sensing tip located close to the samples. Platinum electrodes have been deposited in the specimens either by sputtering under argon in a SCD 040 Balzers equipment or painting with Demetron 308 platinum paste followed by curing at 800°C.

3. Results and discussion

In Table 1 the relative apparent densities of ThO_2:9 mol% Y_2O_3 determined by the Archimedes method are shown according to the preparation method. Theoretical densities have been calculated using cell parameters determined by X-ray diffraction. ThO_2:9 mol% Y_2O_3 powders prepared by the citrate technique sinter to higher than 90% of the theoretical density. For pellets prepared by solid state synthesis, on the other hand; apparent densities lower than 75% of the theoretical density are obtained.

Fig. 1 shows X-ray diffraction spectra of ThO_2:9 mol% Y_2O_3 powders obtained by the citrate technique (Fig. 1a) and of pellets prepared from these powders and sintered at 1550°C/2 h. The main diffraction lines of the thorium oxide fluorite phase are detected, from left to right: [111] 100%, [200] 35%, [220] 58%, [311] 64%, [222] 11%, [400] 8%, [331] 26% and [420] 17%; the number within brackets being the Miller index and the percentages are the relative intensities, respectively.

Table 1
Relative apparent densities of sintered ThO_2:9 mol% Y_2O_3 ceramic specimens obtained by the citrate technique and by solid state synthesis; sintering conditions: 1550°C/2 h

Specimen	Method	%TD
ThO_2:9 mol% Y_2O_3	citrate	91.2
ThO_2:9 mol% Y_2O_3	oxide mixture	72.6

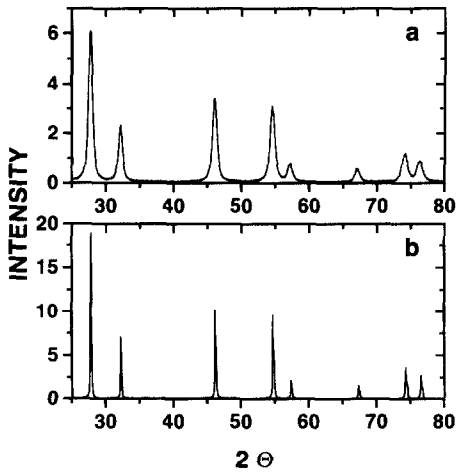

Fig. 1. X-ray diffraction patterns of ThO_2:9 mol% Y_2O_3 powders (a) obtained by the citrate technique and (b) of pellets prepared from these powders and sintered at 1550°C/2 h in air.

Fig. 2 shows results of particle size cumulative distribution analysis of ThO_2:9 mol% Y_2O_3 powders prepared by the citrate technique. The average particle size is 1.1 μm. Both techniques for particle size analysis, using laser and X-rays, are in good agreement. This is indeed a distribution of sizes of particle agglomerates. Stirring the suspension of ThO_2:9 mol% Y_2O_3 powders with sodium hexametaphosphate as deflocculant under ultrasound for several minutes does not break these agglomerates. Transmission electron microscopy (TEM) analysis has been done to look at these agglomerates.

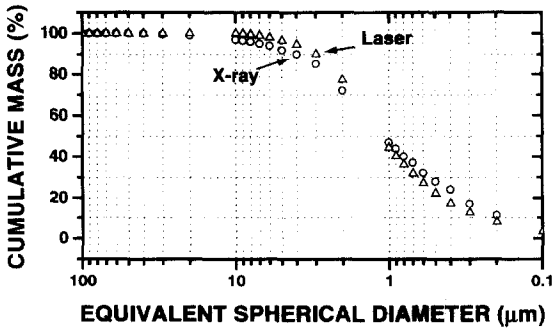

Fig. 2. Cumulative distribution of particle size determined by sedigraphy (X-ray and laser) of ThO_2:9 mol% Y_2O_3 powders prepared by the citrate technique.

Electron microscopy analysis is known as a good complementary technique to look for agglomeration formation. Fig. 3 shows a TEM micrograph of calcined ThO_2:9 mol% Y_2O_3 powders. The powders are composed of a homogeneous distribution of particles with sizes as small as 30 nm. The main feature is that powders obtained by the citrate route are composed of very fine (in the nm range) particles. That explains the relative high densities reached after forming these powders and sintering the ceramic pellets.

Fig. 4a shows the impedance diagram ($-Z'' \times Z'$) measured at 520°C in ThO_2:9 mol% Y_2O_3. The diagram was measured in the 10 Hz–13 MHz frequency range. Two semicircles are easily resolved, one in the low frequency region of the diagrams (10^2 Hz–10^5 Hz) and other in the high frequency region (10^5 Hz–10^7 Hz), hereafter named LF and HF semicircles, respectively. Deconvolution analysis of the diagram of Fig. 4 followed by determination of conductivity values using the geometric factor t/S (t is the specimen thickness and S the electrode area) and the intercept with the real axis gives the following values for the HF semicircle at 520°C: 43×10^{-6} Ω^{-1} cm^{-1} for the conductivity, 10° for the angle below the real axis, and 4.1×10^{-12} F cm^{-1} for the specific capacitance. The corresponding values for the LF semicircle at the same temperature are: 95×10^{-6} Ω^{-1} cm^{-1}, 30° and 4.4×10^{-10} F cm^{-1}. Some conclusions may be drawn from this figure: (a) two easily resolved semicircles are present in the 100 Hz–13 MHz frequency range, due to intragrain (high frequency region) and intergrain (low frequency region) resistivities; (b) the values of capacitance are typical of bulk and grain boundary phenomena for the HF and LF semicircles, respectively [12]; (c) solid solution has been attained otherwise the conductivity of the specimens at that temperature would not be of that order of magnitude (10^{-4} Ω^{-1} cm^{-1}).

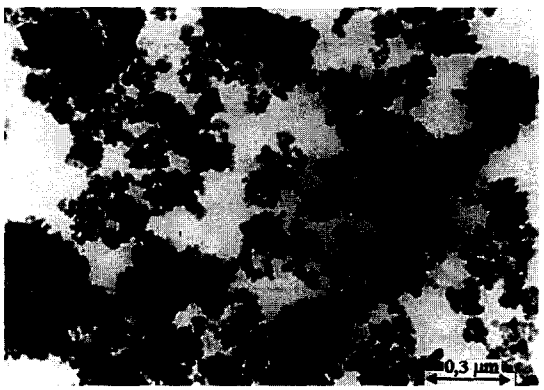

Fig. 3. TEM micrograph of ThO_2:9 mol% Y_2O_3 powders prepared by the citrate technique.

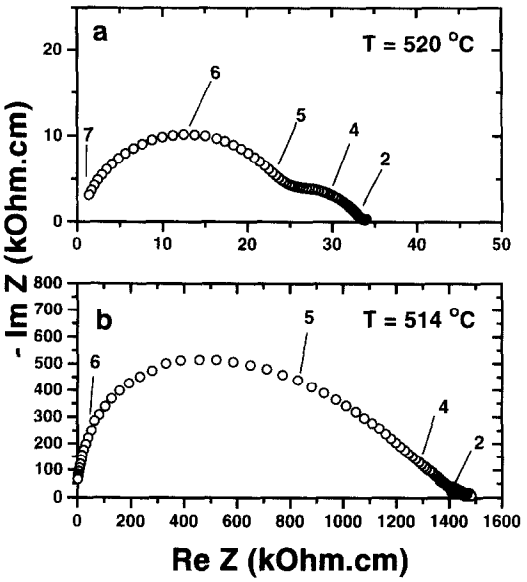

Fig. 4. Impedance diagrams of ThO_2:9 mol% Y_2O_3 sintered ceramic pellets (a) prepared by the citrate technique and (b) by solid state synthesis; temperature of measurement: 520°C (a) and 514°C (b).

In Fig. 4b the impedance diagram measured at 514°C in ThO_2:9 mol% Y_2O_3 sintered ceramic pellet, prepared by mixing the proper amounts of thorium and yttrium oxides, pressing and sintering, is shown. The diagram was measured in the 10 Hz–13 MHz frequency range. Comparing with the diagram of Fig. 4a, several features are evident: (a) the resistivities are more than 30 times larger; (b) the shape of the diagrams is different and their resolution is not straightforward as in the case of the diagrams of ceramic specimens prepared with powders obtained by the citrate technique. The large pore density may play a role in the impedance diagram, acting somehow as a resistive second phase and contributing to the HF semicircle [13,14].

A detailed analysis of the electrochemical impedance spectroscopy research work carried out in thoria–yttria solid solutions is under way [15].

Fig. 5 shows SEM micrographs of ThO_2:9 mol% Y_2O_3 polished and etched sintered pellets obtained by the citrate (a) and the powder mixture techniques (b). Fig. 5a shows a homogeneous distribution of spherical grains of average size 0.3 μm. Typical chemical analysis at points inside the grains in these specimens showed 93.7% of ThO_2 and 6.3% Y_2O_3 corresponding to ThO_2:7.3 mol% Y_2O_3, i.e., for addition of 9 mol% Y_2O_3, approximately 81% go into solid solution. Fig. 5b, on the other hand, shows grains of different average sizes (0.2 μm and 2 μm). EDS analysis inside these grains showed that the large ones have more yttria than the small ones, meaning that grain growth is enhanced by yttria.

4. Conclusions

Reactive thoria–yttria powders have been obtained by the citrate technique. Pellets made using these powders reached higher than 90% of the theoretical density after sintering at 1550°C, a temperature lower than 50% of the melting point of thorium oxide. Electrochemical impedance spectroscopy analyses of these pellets show that they present solid electrolyte behaviour and, consequently, solid solution has been attained. The citrate technique can then be used to produce powders to manufacture thoria–yttria solid electrolytes for oxygen sensing devices.

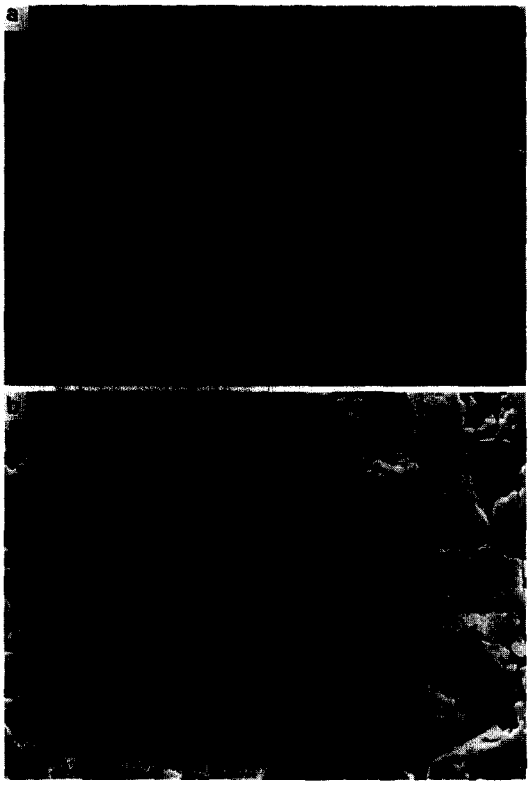

Fig. 5. SEM micrographs of polished and chemically etched ThO_2:9 mol% Y_2O_3 sintered pellets prepared from powders obtained by the citrate technique (a) and bay solid state synthesis (b).

Acknowledgements

Greatly acknowledged are Fundação de Amparo à Pesquisa do Estado de S. Paulo (FAPESP) for financial support and Conselho Nacional de Desenvolvimento Científico e Tecnológico (CNPq) for the scholarship to one of the authors (ICC). Thanks is also due to Selma L. Silva for X-ray measurements, to Celso V. de Morais and Nildemar Ferreira for Electron Microscopy measurements, and to Prof. M. Kleitz of LIES, Grenoble, France for kindly supplying the I.S. software.

References

[1] K.P. Jagannathan, S.K. Tiku, H.S. Ray, A. Ghosh, E.C. Subbarao, Technological applications of solid electrolytes, in: E.C. Subbarao (Ed.), Solid Electrolytes and their Applications, Plenum Press, New York, 1980, p. 201.
[2] N.Q. Minh, J. Am. Ceram. Soc. 76 (1993) 563.
[3] A.K. Mehrotra, H.S. Maiti, E.C. Subbarao, Mat. Res. Bull. 8 (1973) 899.
[4] M. Hartmanová, V. Sály, F. Hanic, M. Pisarcík, H. Ullmann, J. Mat. Sci. 26 (1991) 4313.
[5] R.L. Cook, J.J. Osborne, J.H. White, R.C. MacDuff, A.F. Sammells, J. Electrochem. Soc. 139 (1992) L19.
[6] P. Roy, B.E. Bugbee, Nucl. Technology 39 (1978) 216.
[7] Hj. Matzke, J. Nucl. Mater. 223 (1995) 1.
[8] R. Muccillo, N.H. Saito, E.N.S. Muccillo, Mater. Lett. 25 (1995) 165.
[9] E.C. Subbarao, P.H. Sutter, J. Hrizo, J. Am. Ceram. Soc. 48 (1965) 443.
[10] E. Schouler, A. Hammou, M. Kleitz, Mat. Res. Bull. 11 (1976) 1137.
[11] H.H. Fujimoto, H.L. Tuller, Proc. Int. Conf. Fast Ion Transport in Solids, in: P. Vashishta, J.N. Mundy and G.K. Shenoy (Eds.), Fast ion Transport in Solids, Electrodes and Electrolytes, North Holland, 1979, p. 649.
[12] J.G. Fletcher, A.R. West, J.T.S. Irvine, J. Electrochem. Soc. 142 (1995) 2650.

[13] M. Kleitz, C. Pescher, L. Dessemond, in: S.P.S. Badwal, M.J. Bannister, R.H.J. Hannick (Eds.), Science and Technology of Zirconia V, Technomic Publishing Company, Lancaster, 1993, p. 593.
[14] M.C. Steil, F. Thévenot, L. Dessemond, M. Kleitz, in: P. Duran and J.F. Fernandes (Eds.), Third Euro Ceramics, Vol. 2, Properties of Ceramics, Faenza Editrice Ibérica, San Vincente, 1993, p. 271.
[15] I.C. Cosentino, R. Muccillo, to be published.